ACS APPLIED MATERIALS & INTERFACES

Research Article

www.acsami.org

RoY Peptide-Modified Chitosan-Based Hydrogel to Improve Angiogenesis and Cardiac Repair under Hypoxia

Yao Shu,[†,∥] Tong Hao,[†] Fanglian Yao,[§] Yufeng Qian,[⊥] Yan Wang,[†] Boguang Yang,[†,§] Junjie Li,*[,†] and Changyong Wang*[,†]

[†]Department of Advanced Interdisciplinary Studies, Institute of Basic Medical Sciences and Tissue Engineering Research Center, Academy of Military Medical Sciences, No. 27, Taiping Road, Beijing 100850, China

[§]Department of Polymer Science and Key Laboratory of Systems Bioengineering of Ministry of Education, School of Chemical Engineering and Technology, Tianjin University, Tianjin, 300072, China

[⊥]Department of Chemistry and Biochemistry, University of Texas at Austin, 2500 Speedway, Austin, Texas 78712, United States

[∥]Department of Stomatology, Affiliated Hospital of Academy of Military Medical Sciences, Beijing 100071, China

Supporting Information

ABSTRACT: Myocardial infarction (MI) still represents the "Number One Killer" in the world. The lack of functional vasculature of the infracted myocardium under hypoxia is one of the main problems for cardiac repair. In this study, a thermosensitive chitosan chloride-RoY (CSCl-RoY) hydrogel was developed to improve angiogenesis under hypoxia after MI. First, RoY peptides were conjugated onto the CSCl chain via amide linkages, and our data show that the conjugation of RoY peptide to CSCl does not interfere with the temperature sensitivity. Then, the effect of CSCl-RoY hydrogels on vascularization in vitro under hypoxia was investigated using human umbilical vein endothelial cells (HUVECs). Results show that CSCl-RoY hydrogels can promote the survival, proliferation, migration and tube formation of HUVECs under hypoxia compared with CSCl hydrogel. Further investigations suggest that CSCl-RoY hydrogels can modulate the expression of membrane surface GRP78 receptor of HUVECs under hypoxia and then activate Akt and ERK1/2 signaling pathways related to cell survival/proliferation, thereby enhancing angiogenic activity of HUVECs under hypoxia. To assess its therapeutic properties in vivo, a MI model was induced in rats by the left anterior descending artery ligation. CSCl or CSCl-RoY hydrogels were injected into the border of infracted hearts. The results demonstrate that the introduction of RoY peptide can not only improve angiogenesis at MI region but also improve the cardiac functions. Overall, we conclude that the CSCl-RoY may represent an ideal scaffold material for injectable cardiac tissue engineering.

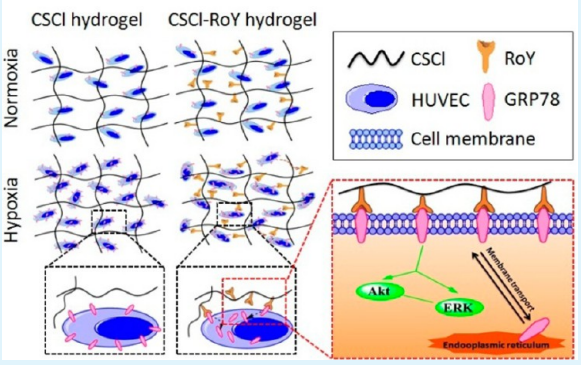

KEYWORDS: *chitosan, RoY peptide, angiogenesis, hypoxia, cardiac tissue engineering*

1. INTRODUCTION

Myocardial infarction (MI) is one of the leading causes of death and disabilities in the world, which can cause irreversible damage to cardiac muscle.[1] Many studies have shown that injectable tissue engineering is an effective method to repair the damaged myocardium.[2−4] Effective vascularization is an important prerequisite for the success of injectable cardiac tissue engineering.[5] In recent years, various injectable hydrogels have been pursued in an attempt to improve the revascularization of MI area, including collagen, matrigel, alginate, chitosan, etc.,[6] which allows for continuous diffusion of nutrients, oxygen, and cells toward the damaged myocardium.[4] In addition, some angiogenic biomolecules (e.g., VEGF, bFGF, HGF, PDGF, etc.) or chemokines (e.g., stromal-derived factor-1) that can stimulate the expression of angiogenic genes were encapsulated in these hydrogels to enhance the matured vessel formation and improve the cardiac function in chronic MI.[7−9] However, the effect of these bioactive factors in promoting angiogenesis was shown to be rather temporary due to their short half-life in vivo.[10] Moreover, the local concentration of bioactive factors is high due to the initial burst release from the hydrogels, which may lead to adverse effects such as the formation of vascular tumors and vascular leakage with edema and hypotension.[11] In addition, their clinical applications are limited owing to their high cost. Therefore, it is important to improve the angiogenic activity of injectable hydrogel for the cardiac repair.

Thermosensitive chitosan-based hydrogels have been widely used in the field of injectable cardiac tissue engineering due to

Received: November 25, 2014
Accepted: March 10, 2015
Published: March 10, 2015

DOI: 10.1021/acsami.5b01234
ACS Appl. Mater. Interfaces 2015, 7, 6505−6517

the unique biocompatibility and controlled biodegradability.[12] Our previous studies showed that the chitosan-based hydrogels can protect the transplanted cells, promote the angiogenesis, reduce infarct size, and improve cardiac function.[13−15] In addition, the amino groups in the backbone allow for conjugation of chitosan with various bioactive molecules,[16] which can increase the bioactive functions without affecting the physical−chemical properties such as gelation behaviors, swelling degree, degradation characteristics, network structure, and mechanical strength.[17] For example, QHREDGS peptide, an integrin binding motif in angiopoietin-1, was covalently immobilized to chitosan hydrogel to support the adhesion of cardiomyocytes.[17,18] In our previous study,[19] chitosan chloride was conjugated with glutathione (GSH), and the produced thermosensitive hydrogels showed excellent antioxidant capacity and biocompatibility to favor the survival of cardiomyocytes under H_2O_2 microenvironment. Therefore, it is possible to develop a chitosan-based hydrogel with good vascularization capacity under hypoxia via peptides modification.

RoY is a 12 amino-acid synthetic peptide (YPHIDSLGHWRR), and it can specifically bind to the 78 kDa glucose-regulated protein (GRP78) receptor, which is largely expressed on membrane surface of vascular endothelial cells under hypoxia. This interaction will then activate the signal pathways related to cell survival and proliferation.[20−23] RoY peptides have been demonstrated to induce angiogenic activity by increasing vascular endothelial cell proliferation, migration, and tube formation under hypoxia in vitro. In addition, local injection of RoY peptide can efficiently alleviate mouse hind limb ischemia.[21,22] Therefore, RoY peptide has a promising application in improving angiogenesis under hypoxic conditions after MI.

In this work, we developed a RoY peptide-modified chitosan chloride hydrogel. The angiogenic property of CSCl-RoY hydrogel under hypoxia was evaluated using human umbilical vein endothelial cells (HUVECs) in vitro. We focused on the roles of CSCl-RoY hydrogel on the survival, proliferation, migration, tube formation of HUVECs, and the related molecular mechanism under hypoxia in vitro. Furthermore, we investigated the effects of CSCl-RoY hydrogel on the angiogenesis and cardiac repair after MI in vivo.

2. MATERIALS AND METHODS

2.1. Peptides Synthesis. RoY (YPHIDSLGHWRR) peptide was synthesized by China Peptides, Shanghai, China. High-performance liquid chromatography (HPLC) and mass spectrometry (MS) analyses suggested that RoY peptide was synthesized successfully and that its purity was over 95%.

2.2. Synthesis and Characterization of Chitosan Chloride−YPHIDSLGHWRR Composites. The synthesis process of CSCl-RoY composites is similar to that for CSCl-GSH composites as in our previous report.[19] Briefly, CSCl (0.5 g, 86% degree of deacetylation, 13.6% hydrochloric acid) was dissolved in 30 mL of deionized water, and a certain amount of RoY and *N*-hydroxysuccinimide (NHS) were dissolved in 10 mL of deionized water according to Table 1. After 30 min, the RoY/NHS solution was added into the CSCl solution under stirring. Then, a certain amount of 1-ethyl-(3, 3-(dimethylamino)-propyl) carbodiimide (EDC) in 10 mL of deionized water was added into the mixture (cf. Table 1) under stirring at room temperature. After 6 h, the mixture was dialyzed against water (molecular weight cutoff: 8kD) for 48 h to remove the unbound reagents. The CSCl-RoY composites with different RoY ratio were obtained after lyophilization. The chemical structure of the CSCl-RoY composites was determined by ^{1}H NMR (INOVA, Varian, USA) using D_2O as the solvent, Fourier transform infrared (FTIR) spectroscopy (MAGNA-560, Nicolet, USA), and differential scanning calorimetry (DSC, METTLER TOLEDO, Switzerland).

Table 1. Reactive Parameter of CSCl-RoY Composites

samples	CSCl (g)	RoY (g)	NHS (g)	EDC (g)
CSCl	0.5			
CSCl-RoY 1	0.5	0.05	0.0055	0.024
CSCl-RoY 2.5	0.5	0.12	0.0055	0.048
CSCl-RoY 5	0.5	0.24	0.0055	0.048

2.3. Preparation and Characterization of Chitosan Chloride−YPHIDSLGHWRR Hydrogels. First, 2% (w/v) CSCl or CSCl-RoY solution in distilled water, 10% (w/v) β-glycerol phosphate (β-GP) solution in distilled water, and 2.5% (w/v) hydroxyethyl cellulose (HEC) solution in Dulbecco's modified Eagle's medium with high glucose were prepared. Second, the CSCl or CSCl-RoY, β-GP, and HEC solutions were quickly mixed according to the volume ratio 5:1.6:1 at room temperature. After incubation at 37 °C for 5−30 min, the CSCl or CSCl-RoY hydrogels were formed. Temperature-sensitivity of CSCl-RoY hydrogel was further studied by measuring the solution viscosity using a rotational viscometer VISCO STAR Plus at 28−40 °C. The gelation time was determined by the test-tube inversion method.[24] Briefly, the mixture of the solutions was incubated at 37 °C, and a time meter was used to record the gelation time when the solution becomes the gel.

2.4. Endothelial Cell Culture. HUVECs were purchased from Sciencell (CA, USA). They were cultured in endothelial cell medium (ECM, Sciencell, USA) containing basal medium, fetal bovine serum (5%), endothelial cell growth supplement, and penicillin/streptomycin in a humidified 37 °C incubator with 5% CO_2 and 21% O_2. The medium was changed every other day. Cell passages were performed using 0.05% trypsin solution when the cells reached 80−90% confluence. HUVECs at passage 3−6 were used in the following experiments.

For seeding into hydogel, HUVECs were first resuspended in β-GP solution. β-GP solution (20 μL) containing HUVECs, 32 μL of HEC solution, and 100 μL of CSCl or CSCl-RoY solution were quickly mixed in 48-well tissue culture plates at room temperature. Then, they were placed in a humidified incubator at 37 °C with 5% CO_2 for preculturing. After 0.5−1 h, HUVECs/CSCl or HUVECs/CSCl-RoY constructs formed, and 0.8 mL of ECM medium was added into each well. The ECM medium was changed every day. For seeding onto the surface of CSCl-RoY hydrogel, the 0.8 mL of culture medium containing a certain number of HUVECs was added into the tissue culture plates covered with CSCl or CSCl-RoY hydrogel.

2.5. Live/Dead Staining. HUVECs/CSCl and HUVECs/CSCl-RoY constructs were cultured in normoxic incubator (21% O_2) or in a hypoxic incubator (Thermofisher Forma 3131, USA) (3% O_2) for 1 and 7 d. The survival of HUVECs in the hydrogels was evaluated using live/dead (Molecular Probes, USA) staining according to manufacturer's instruction and observed using a fluorescence microscopy (Leica, Germany).

2.6. Alamar Blue Assay. HUVECs/CSCl and HUVECs/CSCl-RoY constructs in 48-well plates (5×10^5 cells/constructs) were cultured under normoxia or hypoxia for 1 and 7 d. The proliferation behaviors of HUVECs were measured by Alamar Blue (CellChip Biotechnology, Beijing) assay according to manufacturer's instruction. The percent reduction of Alamar Blue was used to evaluate the proliferative activity of cells. Briefly, cell culture medium was removed at days 1 and 7, and another 300 μL of cell culture medium containing 30 μL of Alamar Blue solution was added. After 12 h, the supernatant (200 μL) was transferred into 96-well tissue-culture plates. Then, the absorbance was measured at a wavelengths of 570 and 600 nm using an enzyme-linked immunosorbent assay plate reader. The percent reduction of Alamar Blue was calculated according to below equation, where $(\varepsilon_{ox})\lambda_2 = 117\,216$, $(\varepsilon_{ox})\lambda_1 = 80\,586$, $(\varepsilon_{RED})\lambda_1 = 155\,677$, and $(\varepsilon_{RED})\lambda_2 = 14\,652$. $A\lambda_1$ and $A'\lambda_1$ are the OD values of the experimental

DOI: 10.1021/acsami.5b01234
ACS Appl. Mater. Interfaces 2015, 7, 6505−6517

and control groups at 570 nm, respectively. $A\lambda_2$ and $A'\lambda_2$ are the OD values of the experimental and control groups at 600 nm, respectively.

$$\text{reduced ratio of Alamar Blue®(\%)} = \frac{(\varepsilon_{ox})\lambda_2 A\lambda_1 - (\varepsilon_{ox})\lambda_1 A\lambda_2}{(\varepsilon_{RED})\lambda_1 A'\lambda_2 - (\varepsilon_{RED})\lambda_2 A'\lambda_1} \times 100$$

2.7. Cell Migration Assay. Transwell permeable support inserts containing a polycarbonate membrane with 8 μm pores (Corning, USA) were first coated with a layer of CSCl or CSCl-RoY hydrogel according to Section 2.3. ECM medium (100 μL) without the serum containing 3×10^4 HUVECs were seeded onto the insets. Then, the insets was transferred into new 24 wells containing 800 μL of ECM medium with 5% fetal bovine serum. After this was cultured for 2 d under normoxia or hypoxia, the migration capacity of HUVECs were investigated via detecting the number of cells through the hydrogels to the bottom sides of the membranes. Briefly, the cells on the membranes were fixed using 4% paraformaldehyde for 30 min at room temperature, and the cell nuclei were stained with 4',6-diamidino-2-phenylindole (DAPI, Sigma, USA) for 15 min. The hydrogels and cells on the top surface of the membranes were carefully wiped out. The bottom-up membranes were transferred to glass slides and mounted using 50 wt % buffering glycerol. The cell nuclei were observed under a fluorescence microscope, and the number of cells adhered on the bottom sides of the membranes was counted using Image-Pro Plus 6.0 software.

2.8. Tube Formation Assay. A 500 μL aliquot of ECM containing 2×10^4 HUVECs was added into 48-well plates covered by CSCl or CSCl-RoY hydrogel, and they were cultured under either normoxia or hypoxia. The morphology of the cells was examined by a light microscopy (Olympus, Japan) every day. At days 4 and 7, 10 randomly chosen visual fields per well were photographed, and the length and area of the network of connected cells (tube formation) were measured using Image-Pro Plus 6.0 software. Tube (capillary-like) formation was defined as a ringlike structure with a length/width ratio of 4.

2.9. Immunofluorescent Staining for GRP78. A 500 μL aliquot of ECM containing approximately 4×10^4 HUVECs was seeded on the surface of CSCl or CSCl-RoY hydrogel in 48-well tissue culture plates and cultured under either normoxia or hypoxia. At day 1, GRP78 protein expression was identified by immunofluorescent staining. Briefly, the cultured HUVECs were fixed in paraformaldehyde (4 wt %) and permeabilized using Triton X-100 (0.3 wt %) for 30 min at room temperature, respectively. After blocking with goat serum (5 wt %), the cells were incubated with rabbit anti-GRP78 antibody (Boster, Wuhan, China) overnight at 4 °C, following by incubation with a fluorescein isothiocyanate (FITC)-conjugated IgG secondary antibody for 2 h at room temperature. Finally, the expression of GRP78 was observed under a fluorescent microscopy.

2.10. Fluorescence Activated Cell Sorting Analysis. GRP78 protein on cell surface was determined by fluorescence-activated cell-sorting analysis (FACS) analysis. Briefly, 2×10^5 cells were seeded on the surface of CSCl or CSCl-RoY hydrogel in six-well culture plates and cultured under normoxia or hypoxia. After 1 d, the cells were dissociated from the hydrogels by TrypLE Express (Gibco, USA). They were incubated with rabbit anti-GRP78 antibody (Boster, Wuhan, China) for 30 min and then incubated with antirabbit FITC-conjugated IgG for another 30 min at room temperature. The control was incubated in phosphate-buffered saline (PBS) instead of anti-GRP78 antibody. Percent of GRP78 positive cells was analyzed by a fluorescence activated cell sorter (FACScan, BD, USA).

2.11. Western Blot Analysis. After 2 d of cultivation under normoxia or hypoxia, HUVECs/CSCl or HUVECs/CSCl-RoY constructs were harvested. The total or membrane proteins were extracted using different Protein Preparation Kit (Applygen, Beijing, China) according to manufacturer's instruction, respectively. The extracted proteins were quantified by BCA Protein Assay Kit (Thermo Scientific, USA). The membrane proteins were loaded on 10−12% sodium dodecyl sulfate (SDS)−polyacrylamide gels. After separated by electrophoresis, they were transferred onto PVDF Western blot membrane. The membrane then was incubated with different primary antibodies (rabbit anti-p-ERK 1/2, p-Akt, ERK 1/2, Akt, Na+-K+ ATPase (Cell Signaling Technology, USA), GRP78, and mouse anti-GAPDH (Boster, Wuhan, China)) overnight at 4 °C, followed by further incubation with appropriate secondary antibodies (goat antimouse and antirabbit IgG (Boster, Wuhan, China)) for 1 h at room temperature. The protein bands were detected by enhanced chemiluminescent reagent (Applygen, Beijing, China) on X-ray films. The band intensity was quantified using Quantity One 4.6.2 software, and normalized to its respective internal standard signal intensity (membrane protein GRP78/Na+-K+ ATPase, other proteins/GAPDH).

2.12. Myocardial Infarction Model and Injection Surgery. Adult male Sprague Dawle (SD) rats were purchased from the Experimental Animal Center at Academy of Military Medical Science (Beijing, China) and were randomly divided into three groups (n = 15 rats/group). MI model was performed as previously described.[25] Briefly, SD rats were intraperitoneally anesthetized with sodium pentobarbital (30 mg/kg) and assisted ventilation during surgery. Limb-lead electrocardiography was performed. Then the heart was exposed via a left lateral thoracectomy and pericardectomy, and the left anterior descending coronary artery was ligated with a 6−0 prolene suture. Subsequently, electrocardiography displayed typical MI waves. After 1.5−2 h when the coronary artery was ligated, 100 μL of PBS, mixture solution of CSCl/CSCl-RoY, β-GP, and HEC was injected along the border of the infarct area at three different locations using a 28-gauge needle. Finally, the chest was closed. The operated rats were fed with standard rat chow and water, individually housed in cages. Above animal experimental procedures were according to the Guide for the Care and Use of Laboratory Animals and approved by the Institutional Animal Care and Use Committee (IACUC) of the Chinese Academy of Military Medical Science (Beijing, China).

2.13. Immunostaining for Blood Vessels. At days 14 and 28 after the injection, animals were euthanatized. The hearts were rapidly excised and fixed using 4% paraformaldehyde for at least 24 h. The heart samples were embedded using paraffin and sectioned through the infarct zone. The sections were incubated with rabbit antivon Willebrand factor (vWF) or mouse anti-α-smooth muscle actin (α-SMA) antibody (Boster, Wuhan, China) overnight at 4 °C and then incubated with antirabbit Cy3-conjugated or antimouse FITC-conjugated IgG for 2 h at room temperature in the dark. Cell nuclei were visualized with DAPI. The sections were observed under a confocal laser microscopy (Olympus, Japan) and analyzed using Image-Pro Plus 6.0 software. Vessel density in infarct zone was measured by counting the number of vWF-positive (vWF+) or α-SMA-positive (α-SMA+) blood vessels per unit area (mm^2). Vessel diameters were measured at the shorter axes of the vessels within the infarct region of the stained sections.[26] Microvessels in each section were defined using the following criteria: positive for vessel labeling within the infarct zone, having a visible lumen and having a diameter between 10 and 100 μm.

2.14. Histology. The infarct size and wall thickness of infarct zone (scar thickness) were assessed using hematoxylin and eosin (HE) staining and Masson's trichrome staining. Infarct size was quantified as the percentage of the length of the infarcted portion in the length of the entire endocardial circumference of left ventricle.[27] Wall thickness was evaluated by measuring the left ventricular wall thickness at evenly spaced locations in the infarct zone.[15,26]

2.15. Echocardiography. Rats were anesthetized at day 28 after the transplantation, and cardiac function was evaluated by echocardiography (14.0 MHz, Sequoia 512; Acuson). Left ventricular shortening fraction (LVFS) and left ventricular ejection fraction (LVEF) were calculated according to the previous report.[15]

2.16. Statistical Analysis. All data were expressed as mean ± standard deviation. The data from the three/five groups in vitro and 15 in vivo were compared, and intergroup differences were analyzed by one-way or two-way ANOVA with Tukey's posthoc test. Statistical analyses were performed with OriginPro 8.0 or SAS 9.0 software. For all analyses, a value of $p < 0.05$ or $p < 0.01$ was accepted as statistically significant.

DOI: 10.1021/acsami.5b01234
ACS Appl. Mater. Interfaces 2015, 7, 6505−6517

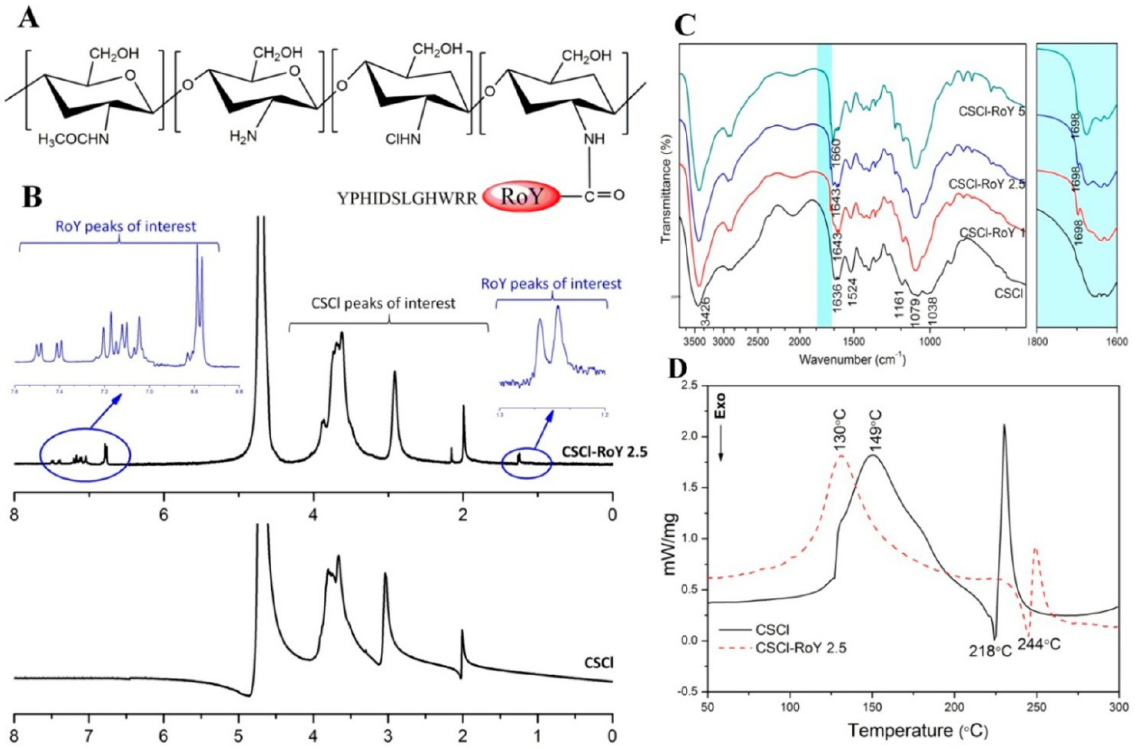

Figure 1. Characterization of CSCl-RoY composites. (A) The chemical structure of CSCl-RoY composites; (B) ^{1}H NMR spectrum, (C) FTIR spectra, and (D) DSC curves of CSCl and CSCl-RoY composites.

3. RESULTS

3.1. Preparation of CSCl-RoY Hydrogels. RoY peptides are coupled to the CSCl chain via the reaction between carboxylic group of the RoY peptide and amino group of the CSCl. As illustrated in Figure 1A, the structure of CSCl-RoY composites is characterized by the amide linkage between the CSCl backbone and the RoY peptide. Three different CSCl-RoY composites were synthesized by varying the CSCl/RoY feeding ratio (cf. Table 1). ^{1}H NMR analysis was performed to confirm the conjugation of the RoY peptide to CSCl chain. As shown in Figure 1B, the chemical shifts at 4.51, 2.93, and 3.64−3.86 ppm belong to proton signals of CSCl. In addition, the spectra of CSCl-RoY composites exhibit additional chemical shifts coming from RoY peptide. For example, the representative proton signals from isoleucine/leucine residues in RoY peptide appear at 1.2−1.3 ppm, and the proton signals within 6.7−7.6 ppm range belong to the tyrosine, tryptophan, and histidine residues of RoY moiety. In addition, FTIR spectroscopy was used to determine the chemical structure of CSCl-RoY composites (Figure 1C). The absorption bands at 1161, 1079, and 1038 cm^{-1} in all samples are assigned to the saccharine structure of CSCl. The characteristic bands at 1636 and 1524 cm^{-1} in CSCl belong to the C−O stretching vibration (amino) and N−H bending vibration (amine), respectively. The carbonyl adsorption bands of RoY peptide appear at 1698 cm^{-1}. Moreover, the absorption band of amine group at 1636 cm^{-1} in the spectra of CSCl shifts to 1660−1643 cm^{-1} in CSCl-RoY composites, indicating that the reaction occurs between carboxylic and amino groups. Therefore, our data confirm that RoY peptides are grafted onto the CSCl chain via the amide linkage. Besides, the intensity of ν(O−H) peak at 3426 cm^{-1} in CSCl-RoY increases compared with that in CSCl, suggesting that there are hydrogen bonds in CSCl-RoY composites and that the interactions enhance in CSCl-RoY compared with that in CSCl. Consistently, the DSC analysis (Figure 1D) shows that CSCl-RoY 2.5 composites have a higher glass transition temperature (149 °C) and thermal degradation temperature (244 °C) than those of CSCl (130 and 218 °C, respectively).

To prepare temperature-sensitive hydrogels, 10% (w/v) β-glycerol phosphate (β-GP) solution in distilled water and 2.5% (w/v) hydroxyethyl cellulose (HEC) were added into CSCl or CSCl-RoY solutions (2%, w/v). The mixture solutions are transparent liquid, which exhibit excellent fluidity at room temperature (Supporting Information, Figure S1A) and can become gel (Supporting Information, Figure S1B) at 37 °C. Supporting Information, Figure S2 shows the viscosity of CSCl and CSCl-RoY solution between 28 and 40 °C; all solutions exhibit low viscosity (ca. 0.1 mPa·S) when the temperature is below 34 °C. However, the viscosity of all CSCl and CSCl-RoY solutions sharply increases at ∼36−37 °C. Moreover, the viscosity of all CSCl-RoY is higher than that of CSCl at 36−37 °C. The viscosity of all CSCl-RoY is more than 1.22 mPa·S at 37 °C, and the viscosity slightly increases with the increase of RoY content in CSCl-RoY. The gelation time of CSCl-RoY hydrogels (8−12 min) is shorter than that of CSCl hydrogel (17.3 ± 6.4 min) at 37 °C.

3.2. Effect of CSCl-RoY Hydrogels on Angiogenic Activity of HUVECs. *3.2.1. Cell Survival and Proliferation.* Survival and proliferation of HUVECs are the prerequisite for vascularization. Our previous studies demonstrated that CSCl-based hydrogels showed an excellent biocompatibility to support the survival and proliferation of many cells.[13,15] We also found that the viability of cardiomyocytes seeded in CSCl hydrogel decreased when they were cultured under the oxidative microenvironment in the presence of H_2O_2.[19] Similar results are found in the present study. As shown in Figure 2A,C, the number of cells in CSCl or CSCl-RoY hydrogel under

DOI: 10.1021/acsami.5b01234
ACS Appl. Mater. Interfaces 2015, 7, 6505−6517

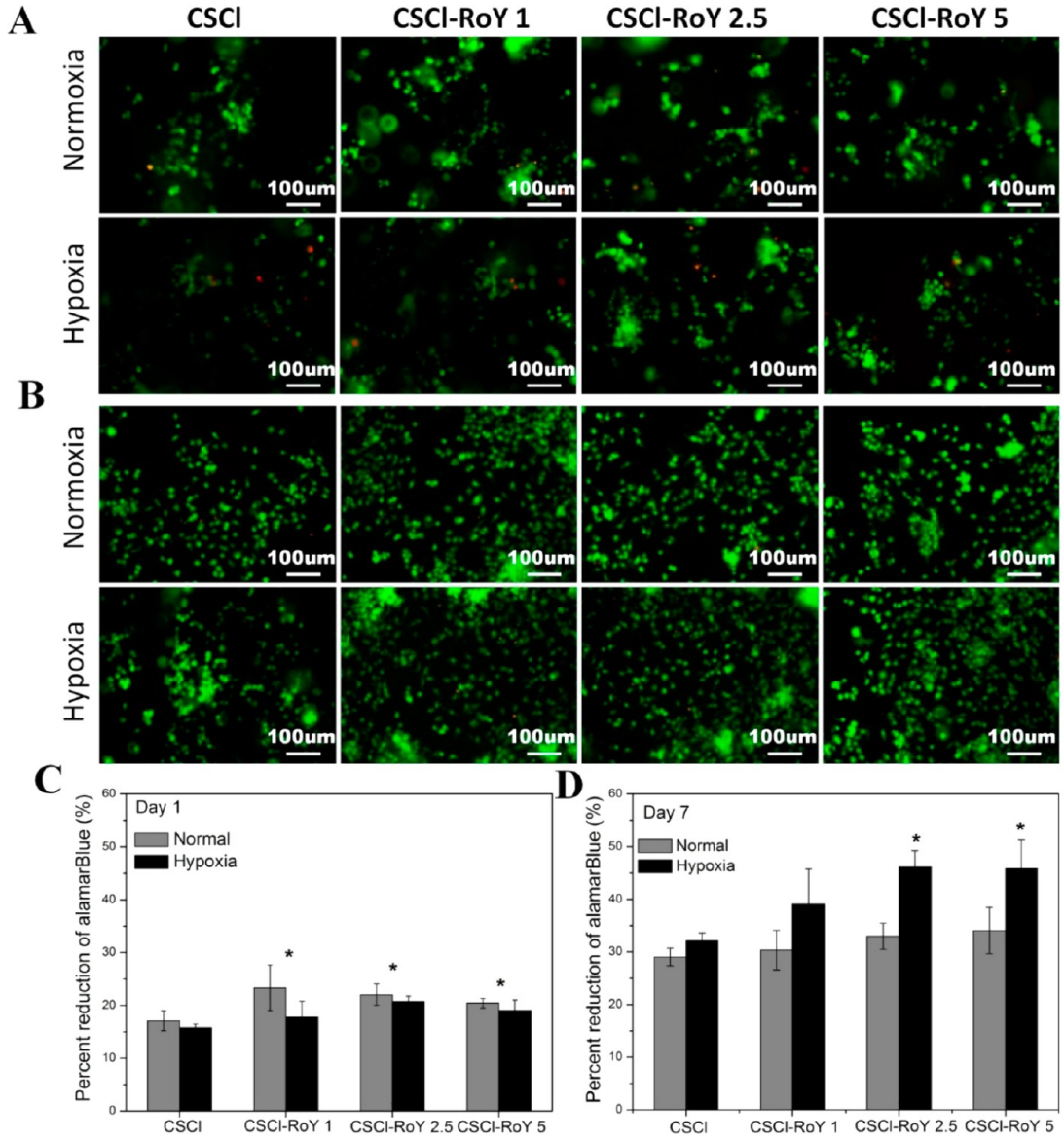

Figure 2. Live/dead staining images of HUVECs cultured in CSCl or CSCl-RoY hydrogels under normoxia or hypoxia at day 1 (A) and day 7 (B). Proliferation behaviors of HUVECs cultured in CSCl or CSCl-RoY hydrogels under normoxia or hypoxia at day 1 (C) and day 7 (D). (* $p < 0.05$ vs CSCl group).

hypoxia is less than that under normoxia at day 1, and a few dead cells (red) can be observed in both CSCl hydrogels and CSCl-RoY hydrogels under hypoxia (Figure 2A). As expect, the number of cells seeded in all hydrogel significantly increase at day 7 (Figure 2). Moreover, the number of cells in CSCl-RoY hydrogels under hypoxia is much more than those in identical hydrogel under normoxia (Figure 2B,D, $p < 0.05$), while the cell number seeded in CSCl hydrogel under hypoxia shows no significant difference ($p > 0.05$) from that of seeded under normoxia. These results suggest that CSCl-RoY hydrogels can better support the survival and proliferation of HUVECs under hypoxia. Furthermore, the proliferative activity of HUVECs seeded in both CSCl-RoY 2.5 and CSCl-RoY 5 hydrogels is much higher than that in CSCl hydrogel ($p < 0.05$) under hypoxia, but there are no statistical differences under normoxia, indicating that the CSCl-RoY hydrogels with moderate/high ratio of RoY are more beneficial for cell proliferation under hypoxia.

3.2.2. Cell Migration. The migration of endothelial cells is an important process during angiogenesis.[28] We examined the migration behaviors of HUVECs through Transwell inserts coated by the hydrogels (Figure 3A). As shown in Figure 3B,C, the combination of RoY into CSCl hydrogel can improve the migration activity of HUVECs under both hypoxia and normoxia. Moreover, the migration capacity of HUVECs enhances with the increase of RoY ratio in CSCl-RoY hydrogels. In addition, results suggest that the different oxygen conditions do not affect the migration performances of HUVECs through CSCl and CSCl-RoY 1 hydrogels ($p > 0.05$). However, the number of HUVECs migrating through CSCl-RoY 2.5 hydrogel under normoxia is more than that under hypoxia ($p < 0.05$). For CSCl-RoY 5 hydrogel with high RoY ratio, the migration capacity of HUVECs under hypoxia is significantly higher than that under normoxia ($p < 0.05$). These results demonstrate that the high RoY ratio in the CSCl-RoY composites can improve the migration of HUVECs under hypoxia.

DOI: 10.1021/acsami.5b01234
ACS Appl. Mater. Interfaces 2015, 7, 6505−6517

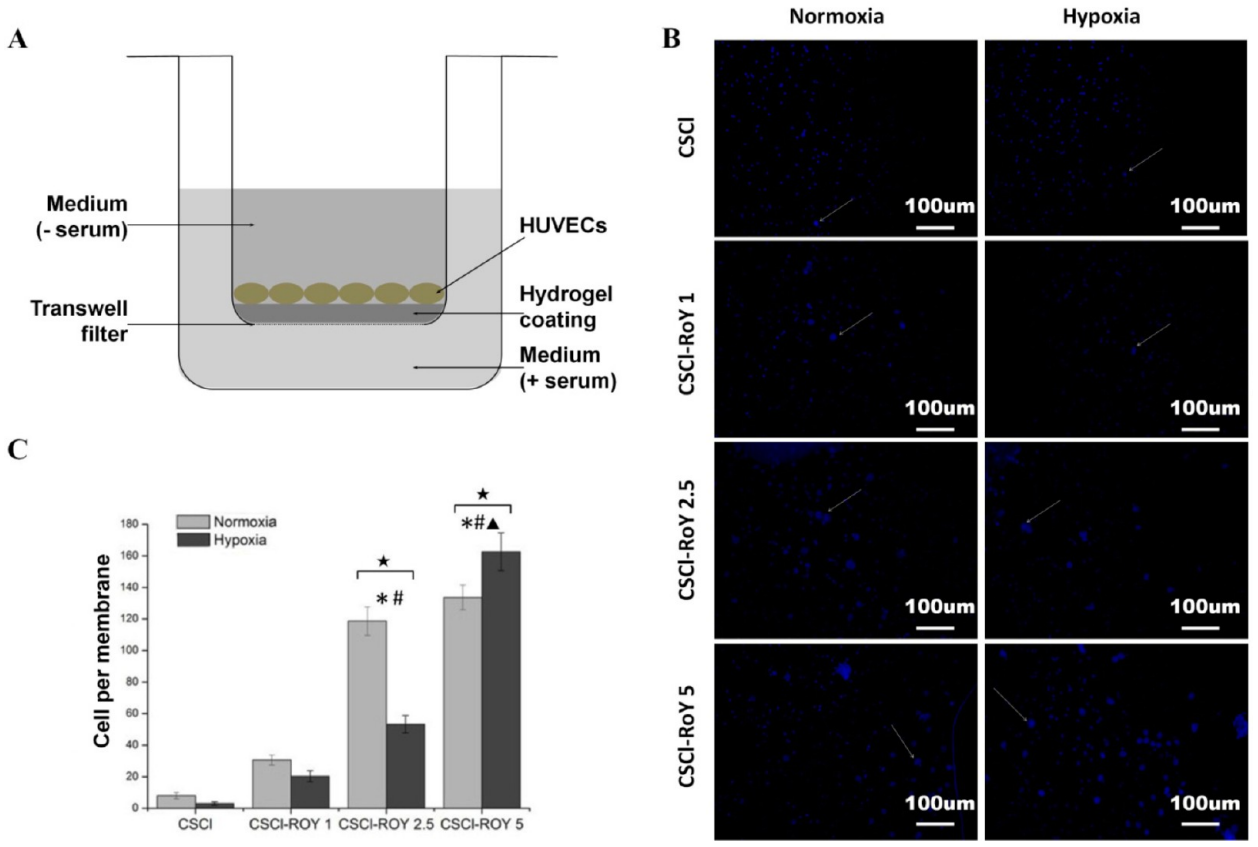

Figure 3. Migration of HUVECs through the CSCl or CSCl-RoY hydrogels under hypoxia or normoxia. (A) Experimental layout of cell migration. (B) Representative images of cells migrating to the bottom of insert membrane (blue: cell nuclei). (C) Quantification analysis of cell migration. (*p < 0.05 vs CSCl, #p < 0.05 vs CSCl-RoY 1, ▲p < 0.05 vs CSCl-RoY 2.5, ★p < 0.05 hypoxia vs normoxia).

3.2.3. Tube Formation. Tube formation, which reflects the vasculogenic potential of endothelial cells, was studied to evaluate angiogenesis in this study. As shown in Supporting Information, Figure S3, HUVECs cultured on the hydrogel surface are organized into a rudimentary capillary-like network comprised of tubelike structures radiating from cell aggregates at day 4. Tubelike structures are not observed on CSCl and CSCl-RoY 1 hydrogel surface under either normoxia or hypoxia, while a few tubes appear on the surface of CSCl-RoY 2.5 and CSCl-RoY 5 hydrogel under hypoxia. At day 7, the network structures are formed on the all-hydrogel surfaces (Figure 4A), and the tubelike structures are more visible with the increase of the RoY in hydrogels. HUVECs on CSCl-RoY 5 hydrogel surface exhibit the clearest lumen-like structures under hypoxia. To further explore the effect of CSCl-RoY hydrogel on the tube formation of HUVECs, the average tube length and tube area at day 7 were analyzed. As shown in Figure 4B,C, there are no statistical differences for both tube length and area between CSCl-RoY hydrogels and CSCl hydrogel group under normoxia (p > 0.05). However, the tube length and area on CSCl-RoY hydrogels are significantly larger than those on CSCl hydrogel under hypoxia (p < 0.05). Moreover, the tube formation capacity of HUVECs on CSCl-RoY 2.5/5 is stronger than that on CSCl-RoY 1 hydrogel. In addition, HUVECs exhibit different tube formation performance under different oxygen conditions. For the CSCl hydrogel, the tube length and area under hypoxia are smaller than that under normoxia. In contrast, HUVECs seeded on CSCl-RoY hydrogel show the improved tube formation capacity under hypoxia compared with that under normoxia. These data suggest that the introduction of RoY is beneficial to induce the tube formation of HUVECs under hypoxia.

3.3. Effect of CSCl-RoY Hydrogel on GRP78 Expression. To investigate the mechanism of angiogenic potential of HUVECs in CSCl-RoY hydrogels under hypoxia, the expression of total GRP78 (t-GRP78) and cell membrane surface GRP78 (s-GRP78) of HUVECs on/in hydrogel were studied. As shown in Figure 5A, many HUVECs cultured on CSCl or CSCl-RoY 5 hydrogel surfaces express GRP78 protein (stained in green) under normoxia. The green fluorescence intensity appears to increase when the cells are incubated under hypoxia, suggesting an increase of t-GRP78 expression in HUVECs. In addition, more than half of the cells seeded on CSCl (54.18%) or CSCl-RoY 5 (58.70%) hydrogel surfaces express the s-GRP78 under normoxia (Figure 5B). However, exposure to 1 d of hypoxia remarkably increases the percent of HUVECs expressing s-GRP78 on CSCl hydrogel (up to 87.96%). In contrast, HUVECs incubated on CSCl-RoY 5 hydrogel under hypoxia induces a significant decrease in s-GRP78 expression (35.86%).

To quantitatively determine the GRP78 expression of HUVECs in different hydrogels, Western blotting of the t-GRP78 and s-GRP78 protein is performed on cells, which were encapsulated in the hydrogels for 2 d of incubation under normoxia or hypoxia. As shown in Figure 5C,D, hypoxia induces a significant increase of t-GRP78 expression level from 0.336 ± 0.002 to 0.653 ± 0.001 and from 0.411 ± 0.003 to 0.677 ± 0.003 for CSCl and CSCl-RoY 5 hydrogel, respectively (p < 0.01). There are no statistical differences in t-GRP78 expression between CSCl and CSCl-RoY 5 hydrogel group

DOI: 10.1021/acsami.5b01234
ACS Appl. Mater. Interfaces 2015, 7, 6505−6517

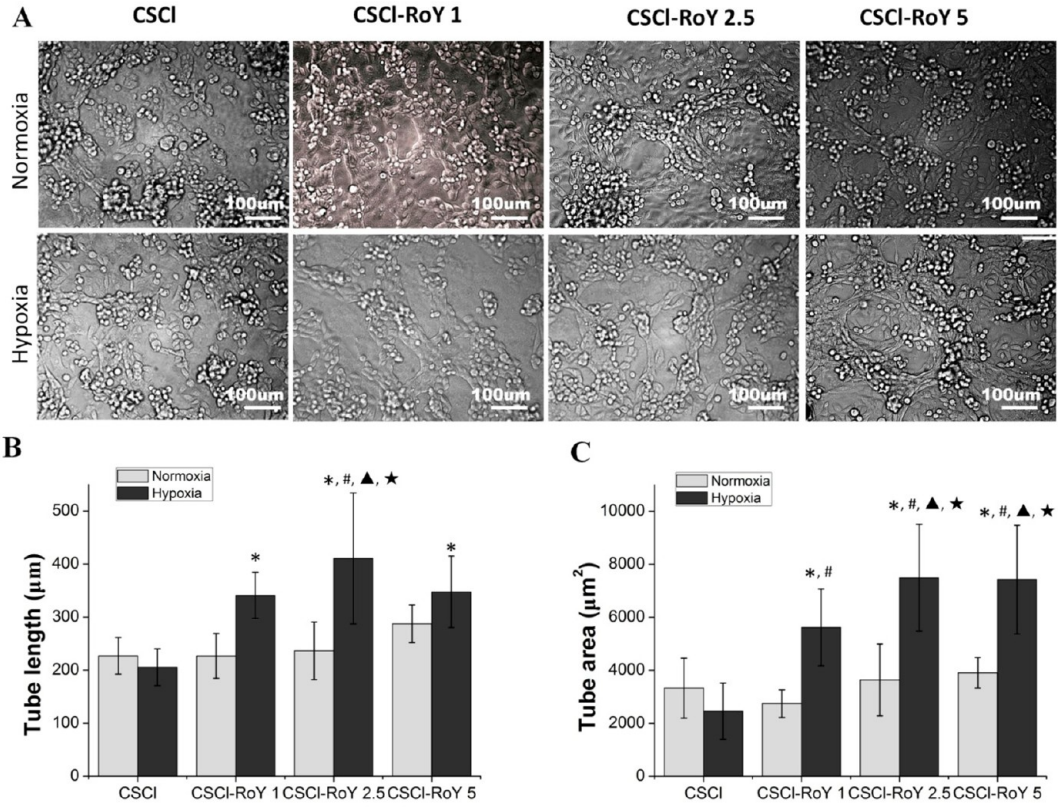

Figure 4. Tube formation of HUVECs cultured on CSCl or CSCl-RoY hydrogels under normoxia or hypoxia. (A) Representative tubelike network structure images of HUVECs cultured on different hydrogel surface at day 7, (B) average tube length, and (C) average tube area. (*$p < 0.05$ vs CSCl, #$p < 0.05$ vs CSCl-RoY 1 under normoxia, ▲$p < 0.05$ vs CSCl-RoY 2.5 under normoxia, ★$p < 0.05$ vs CSCl-RoY 5 under normoxia).

under normoxia ($p > 0.05$). These results are consistent with those of immunofluorescence assay (Figure 5A). For the s-GRP78 (Figure 5C,E), hypoxia significantly increases the s-GRP78 expression level from 0.37 ± 0.02 to 0.80 ± 0.06 in CSCl hydrogel ($p < 0.01$) and from 0.37 ± 0.04 to 0.59 ± 0.05 in CSCl-RoY 5 hydrogel. Notably, the s-GRP78 expression of HUVECs seeded in CSCl-RoY 5 hydrogel (0.59 ± 0.05) is significantly lower than that in CSCl hydrogel (0.80 ± 0.06) under hypoxia ($p < 0.01$), which is consistent with the FACS analysis (Figure 5B). Our data implied that the introduction of RoY peptides to CSCl hydrogel down-regulate the expression of s-GRP78 of HUVECs under hypoxia.

3.4. Effect of CSCl-RoY Hydrogels on Akt and ERK1/2 Phosphorylation. The phosphorylation of Akt (p-Akt) and ERK1/2 (p-ERK1/2) is closely related with cell survival (antiapoptosis) and proliferation. As shown in Figure 6, there are no significant differences in the expression of total Akt and ERK1/2 among all experimental groups. However, the expression of p-Akt and p-ERK1/2 of HUVECs cultured in CSCl hydrogel decreases under hypoxia compared with that under normoxia. Meanwhile, compared to the CSCl hydrogel group, the p-Akt and p-ERK1/2 expression ($p < 0.01$) of HUVECs in CSCl-RoY 5 hydrogel significantly increases under hypoxia, which is close to or slightly lower than the expression level under normoxia (Figure 6B,C). These data suggest that RoY-modified hydrogel can induce the phosphorylation of Akt and ERK1/2 under hypoxia, which might improve the survival and proliferation of HUVECs by activation of the related signal pathways.

3.5. Effect of CSCl-RoY Hydrogels on Angiogenesis in Vivo. The effect of CSCl-RoY hydrogels on angiogenesis in vivo was investigated using immunofluorescence staining with vascular specific antibodies (vWF and α-SMA) at days 14 and 28 after injection surgery. As shown in Supporting Information, Figure S4, some vWF-positive (vWF+) and α-SMA-positive (α-SMA+) blood vessel can be observed at infarct zone at day 14, and the number of neovascularization gradually increases from PBS group to CSCl-RoY 5 hydrogel group. Moreover, the number of α-SMA+ blood vessel is less than that of vWF+ blood vessel. As expected, the number of blood vessels obviously increases (Figure 7A) at day 28, especially in CSCl-RoY 5 group. The further quantification analysis (Figure 7B) shows that both vWF+ and α-SMA+ vessel densities at MI area after the injection of CSCl or CSCl-RoY 5 hydrogel significantly increase compared to PBS group ($p < 0.01$), and the vessel densities in CSCl-RoY 5 group (vWF+: 82.415 ± 8.2/mm^2, α-SMA+: 68.679 ± 7,8/mm^2) are significantly higher than those in CSCl group (vWF+: 63.185 ± 6.5/mm^2, α-SMA +: 43.955 ± 7.8/mm^2) ($p < 0.05$). This indicates CSCl-RoY 5 hydrogel can effectively increase the local vessel density. In addition, the diameter of α-SMA+ blood vessels at MI area after the injection of CSCl (13.12 ± 1.59 μm) or CSCl-RoY 5 (21.13 ± 2.57 μm) hydrogel is bigger than that of PBS group (9.75 ± 1.08 μm, $p < 0.01$, Figure 7C). Moreover, the injection of CSCl-RoY 5 hydrogel significantly increases vWF+ vessel diameter (15.80 ± 1.98 μm) compared with PBS group (9.75 ± 1.08 μm, $p < 0.01$) and CSCl group (13.12 ± 1.59 μm, $p < 0.05$), suggesting that CSCl-RoY 5 hydrogel can promote the vascular formation with greater diameter at MI area.

3.6. Effect of CSCl-RoY Hydrogels on Myocardial Structure and Functions. HE and Masson's trichrome staining were performed to investigate the change of tissue

DOI: 10.1021/acsami.5b01234
ACS Appl. Mater. Interfaces 2015, 7, 6505−6517

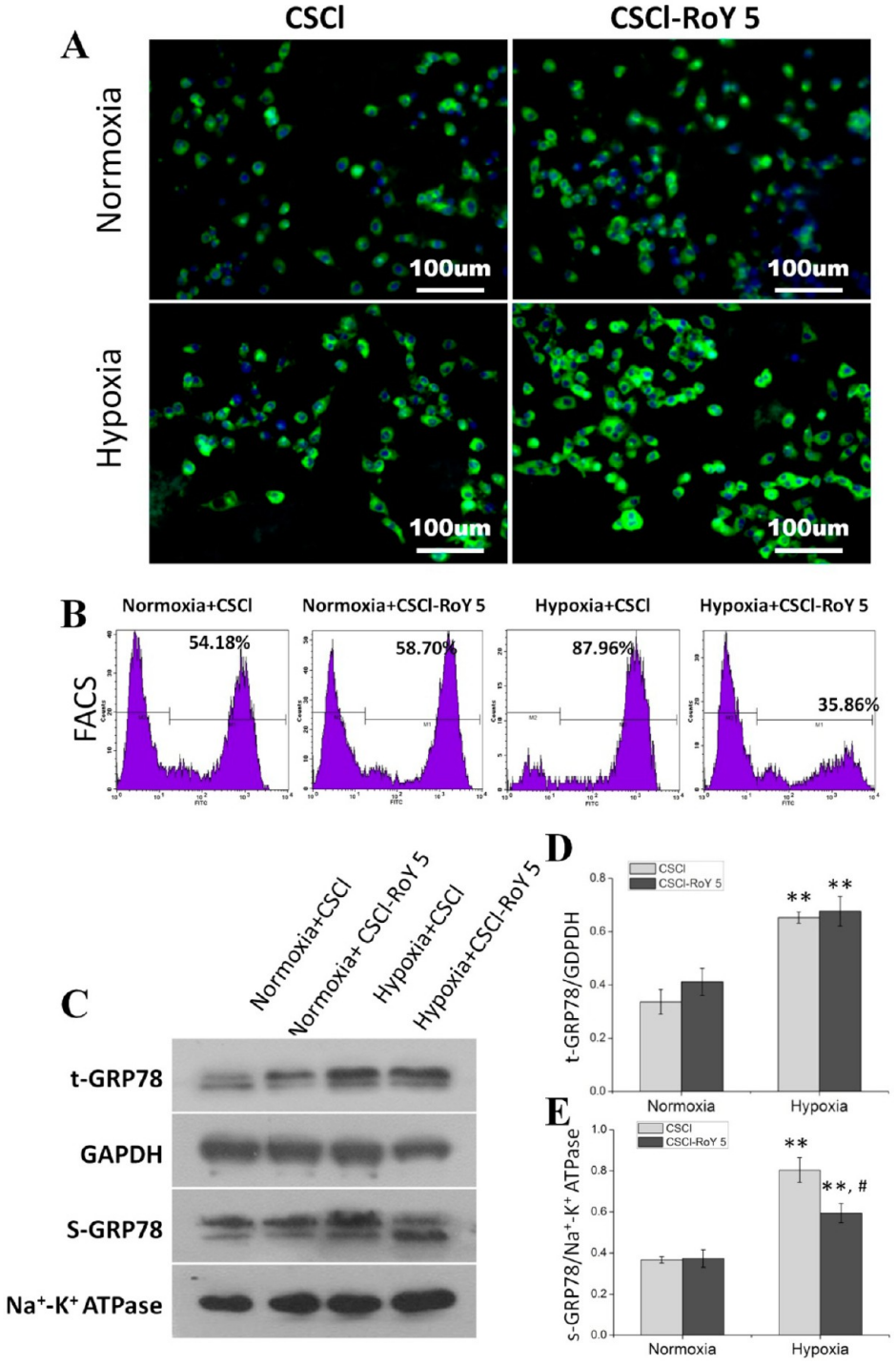

Figure 5. GRP78 expression of HUVECs cultured on/in CSCl or CSCl-RoY 5 hydrogel under normoxia or hypoxia. (A) Immunofluorescence staining t-GRP78 of HUVECs cultured on hydrogel at day 1 (green: GRP78, blue: cell nuclei). (B) FACS analysis of HUVECs expressing s-GRP78 cultured on hydrogel at day 1. (C) Western blot staining of total and cell surface GRP78 of HUVECs cultured in hydrogel at day 2. (D) Quantitative analysis of t-GRP78 (relative to GAPDH). (E) Quantitative analysis of s-GRP78 (relative to Na+-K+ ATPase). t-GRP78: total GRP78; s-GRP78: cell surface GRP78. (** $p < 0.01$ vs normoxia, # $p < 0.01$ vs hypoxia).

structure after MI. HE staining shows that the ventricular wall of MI area is the thinnest after PBS treatment and that the normal cardiac muscle fibers are replaced by connective tissue (Supporting Information, Figure S5A). The thickness of ventricular wall after treatment by CSCl hydrogel obviously increases, but the most cardiac muscle fibers are damaged (Supporting Information, Figure S5B). For the CSCl-RoY 5 group, one can observe many more muscle fibers and blood vessels compared with PBS and CSCl hydrogel groups (Supporting Information, Figure S5C). The Masson's trichrome staining (Figure 8A) shows similar phenomenon, in which infarcted heart, fibroblasts, and collagen exhibit green, while the viable myocardium appears red. Severe fibrosis can be observed in the infarcted hearts after treatment by PBS. The injection of CSCl or CSCl-RoY 5 hydrogel reduces the fibrosis of infarcted myocardium in comparison with the injection of

DOI: 10.1021/acsami.5b01234
ACS Appl. Mater. Interfaces 2015, 7, 6505−6517

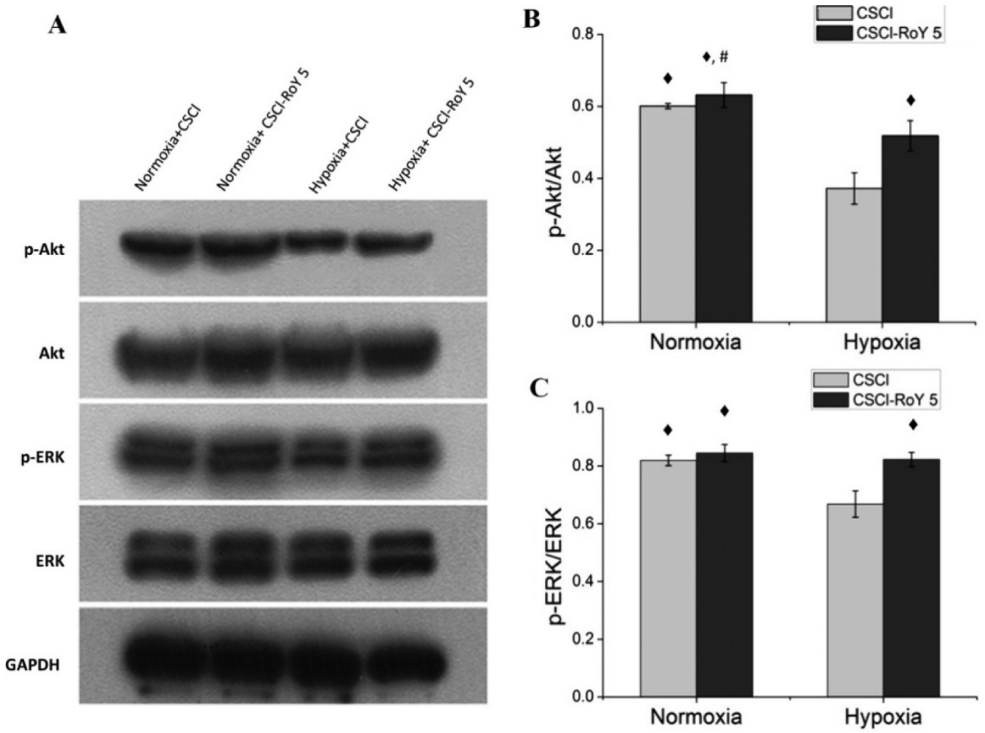

Figure 6. (A) Representative Western blot assay for detecting the levels of Akt, p-Akt, ERK, and p-ERK of HUVECs cultured in CSCl or CSCl-RoY 5 hydrogel under normoxia or hypoxia for 2 d, (B) quantitative analysis of p-AKT levels, and (C) quantitative analysis of p-ERK levels ($\blacklozenge p < 0.01$ vs CSCl group under hypoxia, $^{\#}p < 0.05$ vs CSCl-RoY 5 group under hypoxia).

PBS. The viable myocardium and vascular structures in both center and border of infarct zone are more obvious after treatment by CSCl-RoY 5 hydrogel. Moreover, infarct size significantly decreases by the injection of CSCl-RoY 5 hydrogel compared with the injection of PBS (32.08 ± 2.12% vs 55.85 ± 3.1%, $p < 0.01$) or CSCl hydrogel (32.08 ± 2.12% vs 39.57 ± 2.87%, $p < 0.05$) (Figure 8B). Furthermore, the ventricular wall thickness in the center of infarct zone is 751.79 ± 36.72 μm after treatment by CSCl-RoY 5 hydrogel, which is significantly higher than that after treatment by PBS (559.62 ± 43.30 μm, $p < 0.01$), and had no statistical difference compared with that after treatment by CSCl hydrogel (694.78 ± 42.77 μm, $p > 0.05$, Figure 8C).

The cardiac function is also evaluated at day 28 after the transplantation. As shown in Supporting Information, Figure S6, both LVFS and LVEF are significantly improved in CSCl-RoY 5 group compared with the other groups ($p < 0.01$). These results suggest that the introduction of RoY to CSCl hydrogel could improve the fibrosis of infarcted myocardium, reduce infarct size, increase the ventricular wall thickness of MI area, and improve the cardiac functions.

4. DISCUSSION

Injectable cardiac tissue engineering for MI has shown promising results in animal studies and clinical trials. However, the insufficient revascularization under hypoxic microenvironment of MI zone remains problematic, which may lead to the low survival and growth of host/transplanted cells and affect the recovery of cardiac function. To address these issues, it is necessary to develop novel injectable biomaterial with excellent angiogenic property under hypoxia.[1] Previous studies showed that many cells (e.g., cardiomyocytes,[29] endothelial cells,[23,30] macrophages,[31] etc.) possess self-defense systems to relieve severe stress under ischemia and hypoxia, among which are the overexpression of heat shock proteins including GRP78.[32] More importantly, GRP78, a member of the heat shock protein 70 family, can as a functional receptor on cell surface[21−23] to induce angiogenesis under hypoxia. To improve the angiogenic activity of chitosan-based hydrogel under hypoxia after MI, RoY peptide, a specific ligand of GRP78, is grafted on the CSCl chain via amide linkage in this study, and temperature-sensitive CSCl-RoY-based hydrogel are formed via the electrostatic attractions (between the amino group of chitosan and the phosphate group of β-GP) and hydrophobic interactions (chitosan−chitosan). In this system, RoY can facilitate these interactions and shorten the gelatin time.[19]

Our study shows that more than half of HUVECs seeded on CSCl or CSCl-RoY 5 hydrogel surfaces express the s-GRP78 under normoxia. It is obviously higher than the expression level (24 ± 14%) of HUVECs seeded on tissue culture polystyrene (TCPS) reported by Hardy B et al.[21] We think the overexpression of s-GRP78 under normoxia is to alleviate the oxidative stress damage caused by the hydrogel, because even those biomaterials that are generally considered biocompatible and approved by Food and Drug Administration (e.g., poly(lactic acid)) can induce the oxidative response.[28] Furthermore, the expression of intracellular t-GRP78 significantly increases under hypoxia, which is consistent with GRP78 highly responsive to stress conditions such as hypoxia, as previous studies reported.[33,34] Moreover, the expression of s-GRP78 of HUVECs in/on CSCl hydrogel also increases under hypoxia to protect against the oxidative stress.[30] In contrast, the s-GRP78 expression of HUVECs seeded in/on the CSCl-RoY 5 hydrogel reduces under hypoxia. It is possible that the RoY moiety in CSCl-RoY hydrogel can bind the GRP78 receptor of cell surface and trigger the internalization of s-GRP78 receptor

DOI: 10.1021/acsami.5b01234
ACS Appl. Mater. Interfaces 2015, 7, 6505−6517

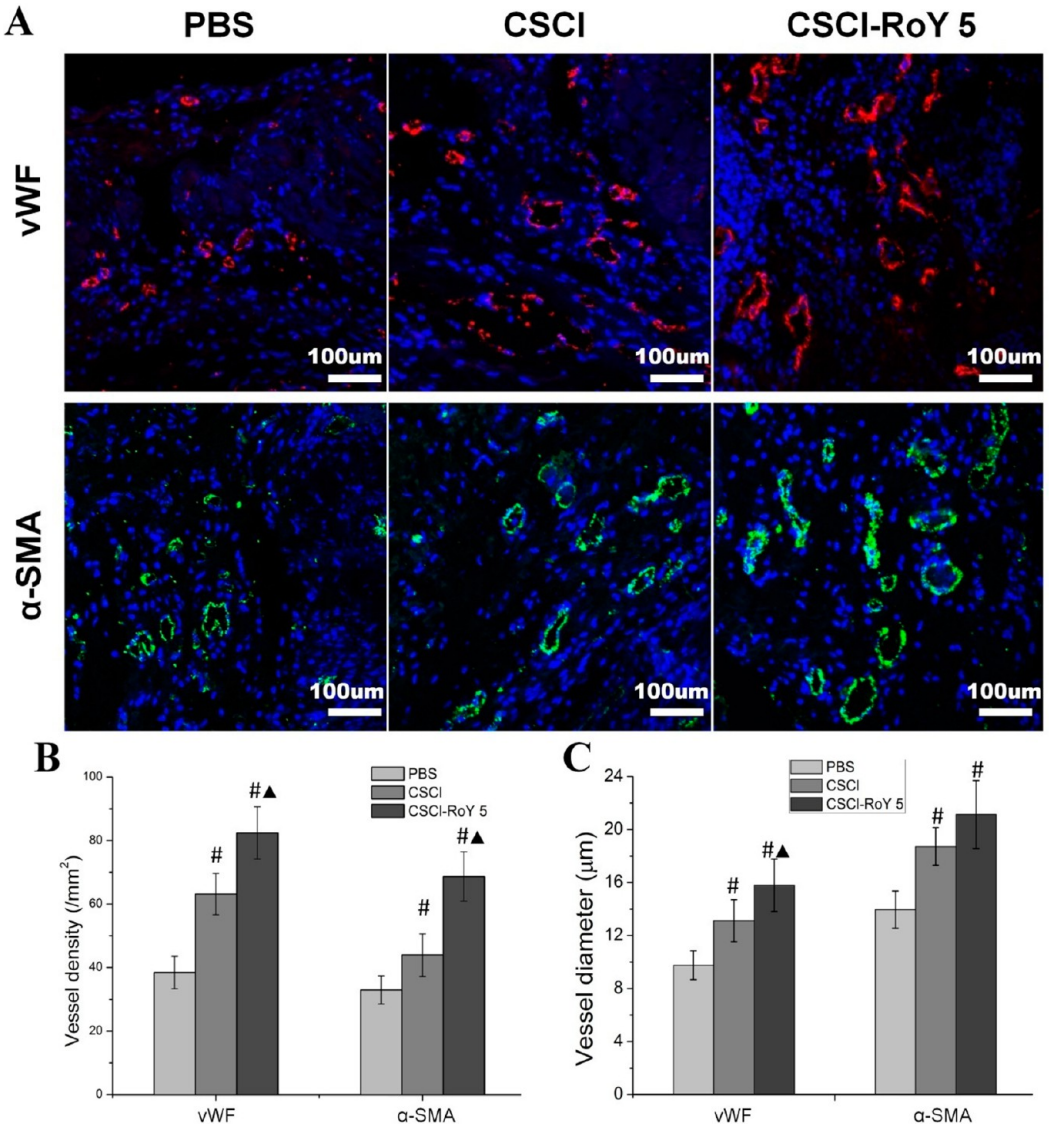

Figure 7. Angiogenesis at infarct zone of MI rat at day 28 after injection surgery. (A) Representative images of myocardial sections from PBS group, CSCl group, CSCl-RoY 5 group stained with vWF (red) or α-SMA (green) antibody. (B) Quantitative analysis of vessel densities with vWF positive or α-SMA positive. (C) Quantitative analysis of vessel diameters with vWF positive or α-SMA positive. ($^{\#}p < 0.01$ vs PBS group, $^{\blacktriangle}p < 0.05$ vs CSCl group).

(cf. Figure 9), leading to a significant decrease of s-GRP78.[23,29,35]

The processes of angiogenesis are complex, typically consisting of cell proliferation, migration, and alignment that result in the formation of tubular structures. This study shows the introduction of RoY to hydrogel can improve the survival and proliferation of HUVECs under hypoxia. The biocompatible chemical nature of chitosan-based hydrogel is one of the main reasons.[12,36] Moreover, there are interactions between RoY ligand in CSCl-RoY hydrogel and GRP78 receptor on HUVECs surface under hypoxia that can induce the internalization of the GRP78 receptor and then might up-regulate the expression of p-Akt and p-ERK1/2 and activate the signaling pathways of cell survival/proliferation (cf. Figure 9).[23,37,38] These results are consistent with previous studies; for example, Gonzalez-Gronow et al.[39] found that the antibodies from prostate patient serum could bind to a segment of membrane GRP78, and then induced prostate cancer cell proliferation.

Our previous study[15] found the injection of CSCl hydrogel could increase the vessel density in ischemic heart. This study found that the injection of CSCl-RoY 5 hydrogel significantly increases the average vessel density and diameter of both vWF+ and α-SMA+ vessels at infarct zone compared with PBS and unmodified CSCl hydrogel. Especially, the increase of α-SMA+ vessels implies an increase of the arterioles or venules supported by pericytes or smooth muscle cells, which are important in maintaining vessel integrity, angiogenesis, and vascular remodeling. These vessels own relatively stable structure and a certain systolic function compared to capillaries with smaller diameter.[40,41] All these characteristics are beneficial to provide the stable vasculature and blood supply for the long-term cardiac repair.[42] In contrast, small capillaries without the supporting cells, which were common in PBS group, may disintegrate with time.[26] Therefore, the CSCl-RoY hydrogel is more favorable for the revascularization of the infarcted myocardium in vivo, which might be caused by following reasons (1) more vascular endothelial cells can migrate into MI

DOI: 10.1021/acsami.5b01234
ACS Appl. Mater. Interfaces 2015, 7, 6505−6517

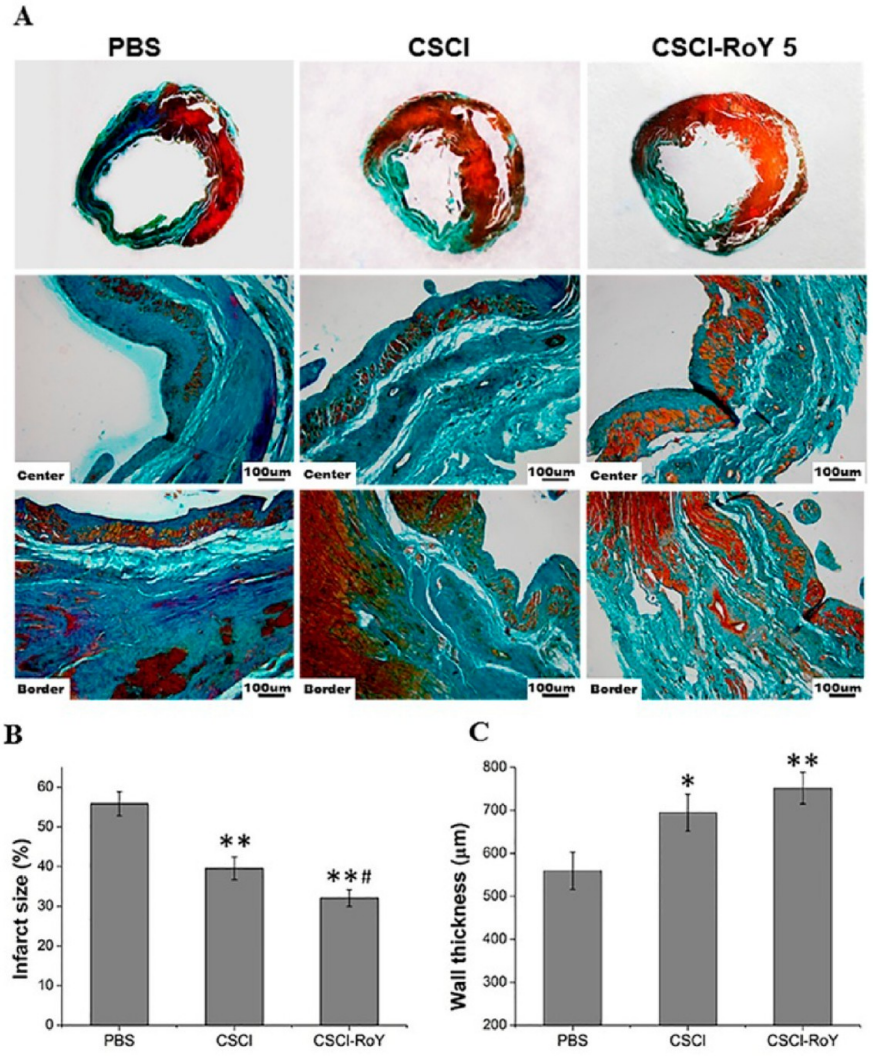

Figure 8. Myocardial structures of infarct zone at day 28 after injection surgery. (A) Representative images of cardiac slices stained with Masson's trichrome staining from PBS group, CSCl group, CSCl-RoY 5 group. (B) Quantitative analysis of infarct size. (C) Quantitative analysis of infarct wall thickness. (*p < 0.05 vs PBS group, **p < 0.01 vs PBS group, #p < 0.05 vs CSCl group).

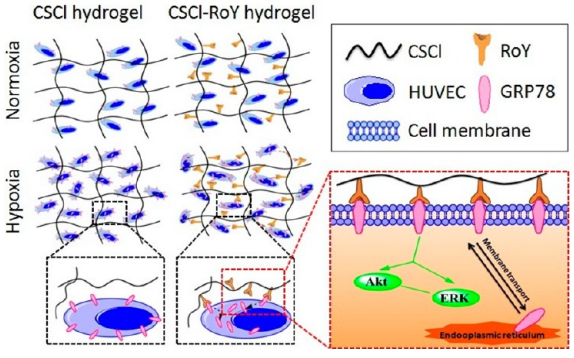

Figure 9. Effect of CSCl-RoY hydrogel on the Akt and ERK signal transduction pathways. The RoY of CSCl-RoY hydrogel can bind the GRP78 receptor of HUVECs under hypoxia and then influence the activation of Akt and ERK signal transduction pathways.

area via the specific interaction between RoY moieties in CSCl-RoY hydrogel and cell surface GRP78 receptors under MI microenvironment, and moreover, the receptor−ligand interactions can further activate the survival/proliferation pathways; (2) CSCl-RoY hydrogel might recruit some angiogenic factors due to the present of amino groups with positive charges.[15,36]

The increase in ventricular wall thickness can reduce the wall stress, prevent wall thinning and dilatation, and further improve heart function. Meanwhile, the decrease of infarct size can attenuate the pathological remodeling, conducive to the recovery of heart function. Here, the results show that the injection of CSCl-RoY 5 hydrogel can increase the wall thickness, reduce the infarct size, and improve the cardiac functions compared with PBS and CSCl hydrogel. We think this is a comprehensive result caused by several factors. First, CSCl-RoY can make more vascular endothelial cells and cardiomyocytes, which expressed GRP78 receptor under MI microenvironment,[30] migrated into MI area, and improved their survival/proliferation capacity via the ligand−receptor interactions. Second, the neovascularization of the infarcted myocardium is enhanced after the injection of CSCl-RoY hydrogel, and then the sufficient blood supply into the infarcted myocardium can further provide the nutrients and oxygen to promote the survival and function of cardiomyocytes. Third, CSCl-based hydrogel provides mechanical support for left ventricle.[15,19] Moreover, the short gelation time of CSCl-RoY

DOI: 10.1021/acsami.5b01234
ACS Appl. Mater. Interfaces 2015, 7, 6505−6517

can make more hydrogel remain in the MI area and furthermore improve the cardiac repair.

5. CONCLUSIONS

To improve the angiogenic property of chitosan-based hydrogel under hypoxia, RoY peptide is grafted onto the CSCl chain via the amide linkages in this study. Results suggest that the CSCl-RoY hydrogel can modulate the expression level of membrane surface GRP78 receptor of HUVECs and then activate Akt and ERK1/2 signaling pathways related to cell survival/proliferation, resulting in improving cell survival, proliferation, migration, and tube formation under hypoxia. Moreover, CSCl-RoY hydrogels can induce angiogenesis at infarct zone in vivo, reduce infarct size, increase wall thickness, and improve the heart functions, leading to the attenuation of myocardial injury and the improvement of cardiac repair. These data provide evidence for the potential applications of CSCl-RoY hydrogel in injectable cardiac tissue engineering.

■ ASSOCIATED CONTENT

Supporting Information

Additional data show images of CSCl-RoY 5, β-GP, and HEC mixed solution at room temperature and at 37 °C; the viscosity of CSCl and CSCl-RoY solution at 28−40 °C; representative images of HUVECs cultured on CSCl or CSCl-RoY hydrogels under normoxia or hypoxia at day 4; angiogenesis at infarct zone of MI rat after injection surgery at day 14; myocardial structures at infarct zone by HE staining at day 14 after injection surgery; echocardiographic results of MI rats at day 28 after hydrogel injection. This material is available free of charge via the Internet at http://pubs.acs.org.

■ AUTHOR INFORMATION

Corresponding Authors

*E-mail: wangchy@bmi.ac.cn or wcy2000_te@yahoo.com. Phone: +86-10-68166874 (C.-Y.W.)

*E-mail: li41308@aliyun.com or li41308@tju.edu.cn. Phone: +86-10-68166874. (J.-J.L.)

Author Contributions

The manuscript was written through contributions of all authors. All authors have given approval to the final version of the manuscript.

Notes

The authors declare no competing financial interest.

■ ACKNOWLEDGMENTS

This work was supported by National Natural Science Funds for Distinguished Young Scholar (No. 31125013), Key Program of National Natural Science Foundation of China (No. 31030032), National Key Basic Research and Development Program of China (No. 2011CB606206), National High Technology Research and Development Program of China (No. 2012AA020506), and National Natural Science Foundation of China (Nos. 31370975, 31100674, 31271016, and 81100782).

■ REFERENCES

(1) Wang, F.; Guan, J. Cellular Cardiomyoplasty and Cardiac Tissue Engineering for Myocardial Therapy. *Adv. Drug Delivery Rev.* **2010**, *62*, 784−797.

(2) Iyer, R. K.; Chiu, L. L.; Reis, L. A.; Radisic, M. Engineered Cardiac Tissues. *Curr. Opin. Biotechnol.* **2011**, *22*, 706−714.

(3) Silva, E. A.; Mooney, D. J. Spatiotemporal Control of Vascular Endothelial Growth Factor Delivery from Injectable Hydrogels Enhances Angiogenesis. *J. Thromb. Haemostasis* **2007**, *5*, 590−598.

(4) Galvez-Monton, C.; Prat-Vidal, C.; Roura, S.; Soler-Botija, C.; Bayes-Genis, A. Cardiac Tissue Engineering and the Bioartificial Heart. *Rev. Esp. Cardiol.* **2013**, *66*, 391−399.

(5) Christman, K. L.; Lee, R. J. Biomaterials for the Treatment of Myocardial Infarction. *J. Am. Coll. Cardiol.* **2006**, *48*, 907−913.

(6) Zhu, J.; He, P.; Lin, L.; Jones, D. R.; Marchant, R. E. Biomimetic Poly(ethylene glycol)-Based Hydrogels as Scaffolds for Inducing Endothelial Adhesion and Capillary-like Network Formation. *Biomacromolecules* **2012**, *13*, 706−713.

(7) Wu, J.; Zeng, F.; Huang, X. P.; Chung, J. C.; Konecny, F.; Weisel, R. D.; Li, R. K. Infarct Stabilization and Cardiac Repair with a VEGF-conjugated, Injectable Hydrogel. *Biomaterials* **2011**, *32*, 579−586.

(8) Ruvinov, E.; Leor, J.; Cohen, S. The Effects of Controlled HGF Delivery from an Affinity-Binding Alginate Biomaterial on Angiogenesis and Blood Perfusion in a Hindlimb Ischemia Model. *Biomaterials* **2010**, *31*, 4573−4582.

(9) Rufaihah, A. J.; Vaibavi, S. R.; Plotkin, M.; Shen, J.; Nithya, V.; Wang, J.; Seliktar, D.; Kofidis, T. Enhanced Infarct Stabilization and Neovascularization Mediated by VEGF-loaded PEGylated Fibrinogen Hydrogel in a Rodent Myocardial Infarction Model. *Biomaterials* **2013**, *34*, 8195−8202.

(10) Yeo, Y.; Geng, W.; Ito, T.; Kohane, D. S.; Burdick, J. A.; Radisic, M. Photocrosslinkable Hydrogel for Myocyte Cell Culture and Injection. *J. Biomed. Mater. Res., Part B* **2007**, *81*, 312−322.

(11) Lee, R. J.; Springer, M. L.; Blanco-Bose, W. E.; Shaw, R.; Ursell, P. C.; Blau, H. M. VEGF Gene Delivery to Myocardium: Deleterious Effects of Unregulated Expression. *Circulation* **2000**, *102*, 898−901.

(12) Ravi Kumar, M. N. A Review of Chitin and Chitosan Applications. *React. Funct. Polym.* **2000**, *46*, 1−27.

(13) Lu, W. N.; Lu, S. H.; Wang, H. B.; Li, D. X.; Duan, C. M.; Liu, Z. Q.; Hao, T.; He, W. J.; Xu, B.; Fu, Q.; Song, Y. C.; Xie, X. H.; Wang, C. Y. Functional Improvement of Infarcted Heart by Co-injection of Embryonic Stem Cells with Temperature-Responsive Chitosan Hydrogel. *Tissue Eng., Part A* **2009**, *15*, 1437−1447.

(14) Wang, H. B.; Zhang, X.; Li, Y.; Ma, Y.; Zhang, Y.; Liu, Z.; Zhou, J.; Lin, Q.; Wang, Y.; Duan, C. M.; Wang, C. Y. Improved Myocardial Performance in Infarcted Rat Heart by Co-Injection of Basic Fibroblast Growth Factor with Temperature-Responsive Chitosan Hydrogel. *J. Heart Lung Transplant.* **2010**, *29*, 881−887.

(15) Liu, Z.; Wang, H.; Wang, Y.; Lin, Q.; Yao, A.; Cao, F.; Li, D.; Zhou, J.; Duan, C. M.; Du, Z. Y.; Wang, Y.; Wang, C. Y. The Influence of Chitosan Hydrogel on Stem Cell Engraftment, Survival and Homing in the Ischemic Myocardial Microenvironment. *Biomaterials* **2012**, *33*, 3093−3106.

(16) Casettari, L.; Vllasaliu, D.; Lam, J. K.; Soliman, M.; Illum, L. Biomedical Applications of Amino Acid-modified Chitosans: A Review. *Biomaterials* **2012**, *33*, 7565−7583.

(17) Reis, L. A.; Chiu, L. L.; Liang, Y.; Hyunh, K.; Momen, A.; Radisic, M. A Peptide-Modified Chitosan-Collagen Hydrogel for Cardiac Cell Culture and Delivery. *Acta Biomater.* **2012**, *8*, 1022−1036.

(18) Rask, F.; Mihic, A.; Reis, L.; Dallabrida, S. M.; Ismail, N. S.; Sider, K.; Simmons, C. A.; Rupnick, M. A.; Weisel, R. D.; Li, R.-K. Hydrogels Modified with QHREDGS Peptide Support Cardiomyocyte Survival in vitro and after Sub-cutaneous Implantation. *Soft Matter* **2010**, *6*, 5089−5099.

(19) Li, J. J.; Shu, Y.; Hao, T.; Wang, Y.; Qian, Y. F.; Duan, C. M.; Sun, H. Y.; Lin, Q. X.; Wang, C. Y. A Chitosan-Glutathione Based Injectable Hydrogel for Suppression of Oxidative Stress Damage in Cardiomyocytes. *Biomaterials* **2013**, *34*, 9071−9081.

(20) Hardy, B.; Raiter, A.; Weiss, C.; Kaplan, B.; Tenenbaum, A.; Battler, A. Angiogenesis Induced by Novel Peptides Selected from a Phage Display Library by Screening Human Vascular Endothelial Cells under Different Physiological Conditions. *Peptides* **2007**, *28*, 691−701.

(21) Hardy, B.; Battler, A.; Weiss, C.; Kudasi, O.; Raiter, A. Therapeutic Angiogenesis of Mouse Hind Limb Ischemia by Novel

DOI: 10.1021/acsami.5b01234
ACS Appl. Mater. Interfaces 2015, 7, 6505−6517

Peptide Activating GRP78 Receptor on Endothelial Cells. *Biochem. Pharmacol.* **2008**, *75*, 891−899.
(22) Raiter, A.; Bechor, Z.; Kleiman, M.; Leshem-Lev, D.; Battler, A.; Hardy, B. Angiogenic Peptides Improve Blood Flow and Promote Capillary Growth in a Diabetic and Ischaemic Mouse Model. *Eur. J. Vasc. Endovasc. Surg.* **2010**, *40*, 381−388.
(23) Raiter, A.; Weiss, C.; Bechor, Z.; Ben-Dor, I.; Battler, A.; Kaplan, B.; Hardy, B. Activation of GRP78 on Endothelial Cell Membranes by an ADAM15-Derived Peptide Induces Angiogenesis. *J. Vasc. Res.* **2010**, *47*, 399−411.
(24) Zhu, W. P.; Gao, L. L.; Luo, Q. J.; Gao, C.; Zha, G. Y.; Shen, Z. Q.; Li, X. D. Metal and Light Free "Click" Hydrogels for Prevention of Post-operative Peritoneal Adhesions. *Polym. Chem.* **2014**, *5*, 2018−2026.
(25) Miyahara, Y.; Nagaya, N.; Kataoka, M.; Yanagawa, B.; Tanaka, K.; Hao, H.; Ishino, K.; Ishida, H.; Shimizu, T.; Kangawa, K.; Sano, S.; Okano, T.; Kitamura, S.; Mori, H. Monolayered Mesenchymal Stem Cells Repair Scarred Myocardium after Myocardial Infarction. *Nat. Med.* **2006**, *12*, 459−465.
(26) Chiu, L. L.; Reis, L. A.; Momen, A.; Radisic, M. Controlled Release of Thymosin β4 from Injected Collagen-Chitosan Hydrogels Promotes Angiogenesis and Prevents Tissue Loss after Myocardial Infarction. *Regener. Med.* **2012**, *7*, 523−533.
(27) Pfeffer, M. A.; Pfeffer, J.M.; Fishbein, M. C.; Fletcher, P. J.; Spadaro, J.; Kloner, R. A.; Braunwald, E. Myocardial Infarct Size and Ventricular Function in Rats. *Circ. Res.* **1979**, *44*, 503−512.
(28) Demirbilek, M. E.; Demirbilek, M.; Karahaliloglu, Z.; Erdal, E.; Vural, T.; Yalcin, E.; Saglam, N.; Denkbas, E. B. Oxidative Stress Parameters of L929 Cells Cultured on Plasma-Modified PDLLA Scaffolds. *Appl. Biochem. Biotechnol.* **2011**, *164*, 780−792.
(29) Hardy, B.; Raiter, A. Peptide-Binding Heat Shock Protein GRP78 Protects Cardiomyocytes from Hypoxia-Induced Apoptosis. *J. Mol. Med. (Heidelberg, Ger.)* **2010**, *88*, 1157−1167.
(30) Davidson, D. J.; Haskell, C.; Majest, S.; Kherzai, A.; Egan, D. A.; Walter, K. A.; Schneider, A.; Gubbins, E. F.; Solomon, L.; Chen, Z.; Lesniewski, R.; Henkin, J. Kringle 5 of Human Plasminogen Induces Apoptosis of Endothelial and Tumor Cells through Surface-Expressed Glucose-Regulated Protein 78. *Cancer Res.* **2005**, *65*, 4663−4672.
(31) Gonzalez-Gronow, M.; Selim, M. A.; Papalas, J.; Pizzo, S. V. GRP78: a Multifunctional Receptor on the Cell Surface. *Antioxid. Redox Signaling* **2009**, *11*, 2299−2306.
(32) Pan, Y. X.; Ren, A. J.; Zheng, J.; Rong, W. F.; Chen, H.; Yan, X. H.; Wu, C.; Yuan, W. J.; Lin, L. Delayed Cytoprotection Induced by Hypoxic Preconditioning in Cultured Neonatal Rat Cardiomyocytes: Role of GRP78. *Life Sci.* **2007**, *81*, 1042−1049.
(33) Hayashi, T.; Saito, A.; Okuno, S.; Ferrand-Drake, M.; Chan, P. H. Induction of GRP78 by Ischemic Preconditioning Reduces Endoplasmic Reticulum Stress and Prevents Delayed Neuronal Cell Death. *J. Cereb. Blood Flow Metab.* **2003**, *23*, 949−61.
(34) Pan, Y. X.; Lin, L.; Ren, A. J.; Pan, X. J.; Chen, H.; Tang, C. S.; Yuan, W. J. HSP70 and GRP78 Induced by Endothelin-1 Pretreatment Enhance Tolerance to Hypoxia in Cultured Neonatal Rat Cardiomyocytes. *J. Cardiovasc. Pharmacol.* **2004**, *44* (Suppl 1), S117−S120.
(35) Gonzalez-Gronow, M.; Kaczowka, S. J.; Payne, S.; Wang, F.; Gawdi, G.; Pizzo, S. V. Plasminogen Structural Domains Exhibit Different Functions when Associated with Cell Surface GRP78 or the Voltage-Dependent Anion Channel. *J. Biol. Chem.* **2007**, *282*, 32811−32820.
(36) Gao, J. S.; Liu, R. F.; Wu, J.; Liu, Z. Q.; Li, J. J.; Zhou, J.; Hao, T.; Wang, Y.; Du, Z. Y.; Duan, C. M.; Wang, C. Y. The Use of Chitosan Based Hydrogel for Enhancing the Therapeutic Benefits of Adipose-Derived MSCs for Acute Kidney Injury. *Biomaterials* **2012**, *33*, 3673−3681.
(37) Misra, U. K.; Deedwania, R.; Pizzo, S. V. Activation and Cross-talk between Akt, NF-kappaB, and Unfolded Protein Response Signaling in 1-LN Prostate Cancer Cells Consequent to Ligation of Cell Surface-Associated GRP78. *J. Biol. Chem.* **2006**, *281*, 13694−13707.
(38) Kelber, J. A.; Panopoulos, A. D.; Shani, G.; Booker, E. C.; Belmonte, J. C.; Vale, W. W.; Gray, P. C. Blockade of Cripto Binding to Cell Surface GRP78 Inhibits Oncogenic Cripto Signaling via MAPK/PI3K and Smad2/3 Pathways. *Oncogene* **2009**, *28*, 2324−2336.
(39) Gonzalez-Gronow, M.; Cuchacovich, M.; Llanos, C.; Urzua, C.; Gawdi, G.; Pizzo, S. V. Prostate Cancer Cell Proliferation in vitro is Modulated by Antibodies Against Glucose-Regulated Protein 78 Isolated from Patient Serum. *Cancer Res.* **2006**, *66*, 11424−11431.
(40) Chiu, L. L.; Reis, L. A.; Momen, A.; Radisic, M. Controlled Release of Thymosin β4 from Injected Collagen−Chitosan Hydrogels Promotes Angiogenesis and Prevents Tissue Loss after Myocardial Infarction. *Regener. Med.* **2012**, *7*, 523−533.
(41) Chu, H. H.; Gao, J.; Chen, C. W.; Huard, J.; Wang, Y. D. Injectable Fibroblast Growth Factor-2 Coacervate for Persistent Angiogenesis. *Proc. Natl. Acad. Sci. U. S. A.* **2011**, *108*, 13444−13449.
(42) Chu, H.; Chen, C. W.; Huard, J.; Wang, Y. The Effect of a Heparin-Based Coacervate of Fibroblast Growth Factor-2 on Scarring in the Infarcted Myocardium. *Biomaterials* **2013**, *34*, 1747−1756.

DOI: 10.1021/acsami.5b01234
ACS Appl. Mater. Interfaces 2015, 7, 6505−6517